ISSN 1070-3632, Russian Journal of General Chemistry, 2015, Vol. 85, No. 3, pp. 692–707. © Pleiades Publishing, Ltd., 2015.

Spectroscopic and Anticancer Studies on New Synthesized Copper(II) and Manganese(II) Complexes with 1,2,4-Triazines Thiosemicarbazide[1]

Moamen S. Refat[a,b], I. M. El-Deen[b], M. S. El-Garib[b], and W. Abd El-Fattah[b]

[a] *Department of Chemistry, Faculty of Science, Taif University, Al-Hawiah, Taif, P.O. Box 888 Zip Code 21974, Saudi Arabia*
[b] *Department of Chemistry, Faculty of Science, Port Said University, Port Said, Egypt*
e-mail: msrefat@yahoo.com

Received December13, 2014

Abstract—Binuclear Cu(II) and Mn(II) newly transition metal complexes of the 5-benzylidene-3-(4-chloro-phenyl)-6-oxo-5,6-dihydro-1*H*-[1,2,4]triazine-2-carbothioic acid amide (HL^1) and 5-(3-bromo-4-methoxy-benzylidene)-3-(4-chloro-phenyl)-6-oxo-5,6-dihydro-1*H*-[1,2,4]triazine-2-carbothioic acid amide (HL^2) derived from the condensation of oxazolinone with thiosemicarbazide have been prepared. The structural elucidation was discussed upon elemental analyses and molar conductivity, as well as from mass, ^{1}H NMR, IR, UV-Vis spectral studies. From the analytical, spectroscopic and thermal data, the stoichiometry of the mentioned complexes was found to be 1 : 2 (metal : ligand). The molar conductance data revealed that all the metal chelates are non-electrolytes and the sulphato ions existing inside of the coordination sphere. The thermal stabilities of these complexes were studied by thermogravimetric (TG-DTG/DTA) and the decomposition steps of these complexes are investigated. The kinetic thermodynamic parameters such as the energy of activation (E*), pre-exponential factor (A), activation entropy (ΔS*), activation enthalpy (ΔH*) and free energy of activation (ΔG*) have been calculated. Inhibitory activity against breast carcinoma cells (MCF-7 cell line), hepatocellular carcinoma cells (HePG-2 cell line) and colon carcinoma cells (HCT cell line) were tested by using different concentrations of the samples (50, 25, 12.5, 6.25, 3.125, and 1.56 μg) and cell viability (%) was determined by colorimetric method. The drug doxrubcin was used as standard.

Keywords: 1,2,4-triazines, thiosemicarbazide, transition metals, thermal analysis, anticancer

DOI: 10.1134/S1070363215030299

INTRODUCTION

Metal complexes of N (nitrogen) and S (sulfur) chelating ligands have attracted considerable attention [1] because of their interesting physicochemical properties, pronounced biological activities and as models of the metalloenzyme active sites. It is well known that N and S atoms play a key role in the coordination of metals at the active sites of numerous metallobiomolecules. Schiff-base metal complexes [2–5] have been widely studied because they have industrial, antifungal, antibacterial, anticancer and herbicidal applications. They serve as models for biologically important species and find applications in biomimetic catalytic reactions. Chelating ligands containing N and S as donor atoms [6, 7] show broad biological activity [8–11] and are of special interest because of the variety of ways in which they are bonded to metal ions [12]. It is known that the existence of metal ions bonded to biologically active compounds may enhance their activities.

Triazine derivatives have traditionally found applications in analytical chemistry as complexation agents, in electrochemistry as multi-step redox systems and as pesticide or herbicide components in agriculture. They [13] are known to possess antitubercular, antibacterial, fungicidal, hypotensive and hypothermic activities. Numerous compounds containing the 1,2,4-triazine moieties are well known in natural materials and show biological, pharmacological and medicinal properties. An interesting characteristic of the derivatives of 1,2,4-triazine compounds is that they form colored complexes when they are coordinated to a metal ion. In particularly, the ligand 5,6-diphenyl-3-

[1] The text was submitted by the authors in English.

(2-pyridyl)-1,2,4-triazine, noted dppt, has been widely used as an sensitive reagent for the determination of Fe(II) by spectrophotometric methods, in natural and waste waters [14]. Its role as transfer agent for transition metal ions has been showed by electrochemistry studies [15]. Some Cu(II) complexes have been isolated and studied as potential catalytically active redox agents [16]. More recently, it has been revealed that a zinc–dppt complex associated to a biocide could have significant biocidal effects on living cells including those of microorganisms (bacteria and fungi), cell culture system, plants and animals [17]. Elena et al., [18] studied the synthesis and characterization of Cd(II), Zn(II), Pb(II), Co(III), and Ni(II) complexes of 5-methoxy-5,6-diphenyl-4,5-dihydro-2*H*-[1,2,4]triazine-3-thione (LH_2OCH_3). The stoichiometry of the complexes was found to be 1 : 2 except for cobalt complex, where the ratio is 1 : 3. In all complexes the triazine is deprotonated and acts at least as a NS bidentate ligand. The complexes have been characterized by microanalysis, mass spectrometry, IR, multinuclear (^1H and ^{13}C) NMR, ^{13}C CP/MAS NMR and magnetic susceptibility. In addition, the structure of the complex $[Cd(DMF)L_2]_2 \cdot 2DMF \cdot 1/4H_2O$, has been determinedby X-ray diffraction. Crystallographic data show that the complex consists of a dinuclear structure, in which the ligands act as bidentate NS donors and with two of the four ligands acting as a bridge between the metal ions via the sulfur atom. A similar study [19] was carried out by using a series of cobalt, nickel, copper, and zinc complexes of bidentate Schiff base derived from the condensation of 5-bromothiophene-2-carboxaldehyde with 4-amino-3-mercapto-6–methyl-5-oxo-[1,2,4] triazine. The Schiff base exhibits a strong fluorescence emission, contrast to this partial fluorescence quenching phenomena is observed in its metal complexes. The Schiff base and its metal complexes have been screened for antibacterial (*Staphylococcus aureus*, *Bacillus subtilis*, *Escherichia coli*, *Pseudomonas aeruginosa*) and antifungal activities (*Aspergillus niger* and *A. flavus*).

Furthermore, the coordination behavior of the triazine ligand with NNO donation sites, derived from 3-benzyl-7-hydrazinyl-4*H*-[1,3,4]thiadiazolo[2,3-*c*][1,2,4]triazin-4-one, towards some metal ions namely Mn(II), Fe (III), Co(II), Ni(II), Cu(II), and Zn(II) was reported [20]. The synthesized ligand and its metal complexes were found to have biological activity against the desert locust *Schistocerca gregaria* (Forsk.) (*Orthoptera–Acrididae*) and, its adult longevities derived from thiocarbohydrazide, exhibits biological activity, such as antiviral, antimalarial and antifungal [21], and exists in two thione and thiole tautomeric forms. Therefore, it may coordinate either as a neutral ligand via its S atom [22] or (by loss of a proton) anionic N–S bidentate ligand. Mitra et al. [23] studied the reaction of 4-amino-6-methyl-1,2,4-triazine-3-thione-5-one (AMTTO, **I**) with platinum(II) chloride in THF led to the platinum complex $[(AMTTO)PtCl_2]_3 \cdot 4.5THF$ in excellent yields.

In continuity, dinuclear complexes $[\{Pt(trpy)\}_2(L)] \cdot (PF_6)_2$ (trpy = 2,2':6',2''-terpyridine, L = 2-octylthio-1,3,5-triazine-4,6-dithiolate ion, L = 2-octadecylthio-1,3,5-triazine-4,6-dithiolate ion, L = 2-di-*n*-butylamino-1,3,5-triazine-4,6-dithiolate ion) and a trinuclear complex $[\{Pt(trpy)\}_3(L)](PF_6)_3$ (L = 1,3,5-triazine-2,4,6-trithiolate ion) have been synthesized and characterized [24].

The reactions of 5,6-diphenyl-3-(2-pyridyl)-1,2,4-triazine with $CuCl_2 \cdot 2H_2O$, $Cu(NO_3)_2 \cdot 3H_2O$, and $CuSO_4 \cdot 5H_2O$ have been examined by Machura et al. [25] and four $[CuCl_2(dppt)]$, $[CuCl_2(dppt)_2] \cdot 2MeOH$, $[Cu(dppt)_2(H_2O)_2](NO_3)_2$ and $[Cu(SO_4)(dppt)(H_2O)]_n \cdot nH_2O$ complexes have been obtained.

Bereau et al. [26] synthesized the copper(II) and nickel(II) complexes of 5,6-diphenyl-3-(2'-hydroxyphenyl)-1,2,4-triazine, noted HL_H, and 5,6-bis(4-methoxyphenyl)-3-(2'-hydroxyphenyl)-1,2,4-triazine, noted HL_{OMe} from copper(II) acetate in CH_2Cl_2 and nickel(II) nitrate in acetone with an excess of previously deprotonated triazine. The new complexes $[Cu(L_H)_2] \cdot H_2O$ (**I**), $[Cu(L_{OMe})_2] \cdot 2H_2O$ (**II**), $Na[Ni(L_H)_3] \cdot 2H_2O \cdot (CH_3)_2CO$, and $Na[Ni(L_{OMe})_3] \cdot 2H_2O$ were isolated as pure solids and characterized by IR, UV-Vis, elemental analysis and mass spectra.

Kiran et al. [27] isolated a few (1 : 1) and (1 : 2) metal complexes of cobalt(II), nickel(II), copper(II) and zinc(II) with ligand derived from the condensation of 4-amino-3-mercapto-6-methyl-5-oxo-1,2,4-triazine with 2-acetylpyridine. Some of the chemically synthesized compounds have been screened in vitro against the three Gram-positive (*Staphylococcus aureus, Staphylococcus epidermidis* and *Bacillus subtilis*) and two Gram-negative (*Salmonella typhi and Escherichia coli*) organisms. It is observed that the coordination of metal ion has pronounced effect on the microbial activities of the ligand. The metal complexes have higher antimicrobial effect than the free ligands.

Scheme 1. Preparation pathway of HL^1 and HL^2 free ligand

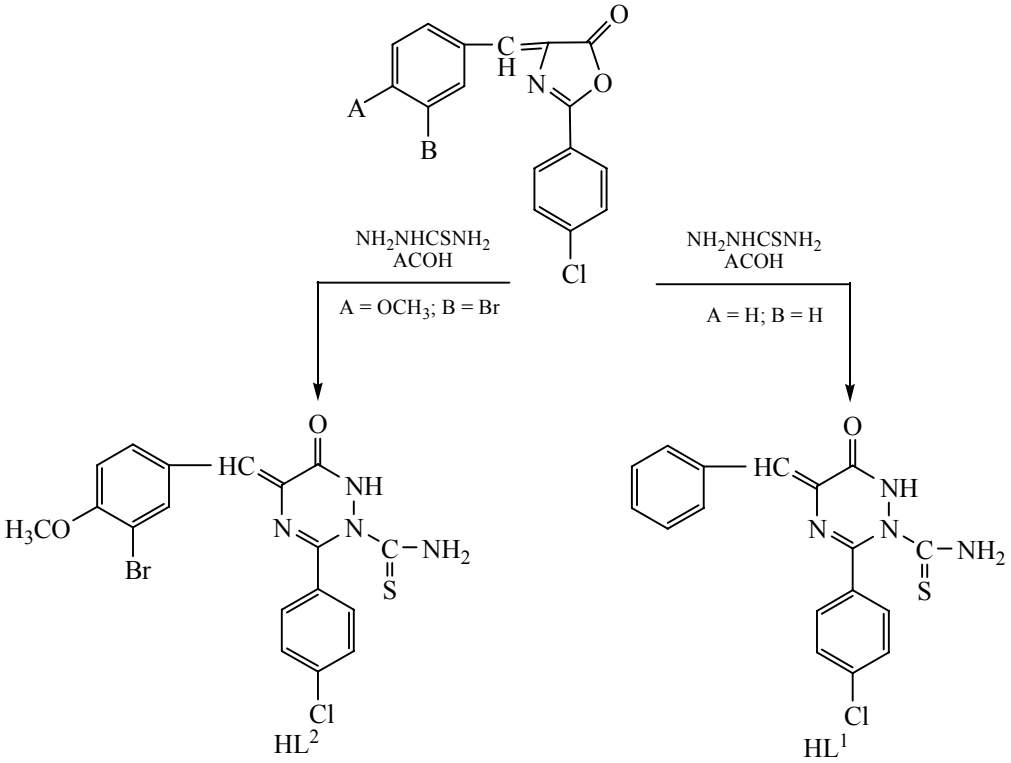

Thiosemicarbazones usually act as chelating ligands with a transition metal ion, bonding through the sulphur and hydrazine nitrogen atoms. Also, compounds containing O, S and N atoms and their complexes have received considerable attention because of their pharmacological activities [28]. The metal complexes show more activities as compared to the free thiosemicarbazides. They show numerous applications [29–31] particularly with the first row of transition metal complexes. In view of above applications it is highly desirable to synthesize and characterize transition metal complexes with such ligands. The structure of the thiosemicarbazide moiety confers a good chelating capacity and this property can be increased in thiosemicarbazone by inserting suitable aldehyde or ketone possessing further donor atoms to render the ligand polydentate [32]. The Varity of possible Schiff bases metal complexes with wide choice of ligands and coordination environments has prompted us to undertake research in this area [33]. In the present work we report the synthesis and characterization of Cu(II) and Mn(II) complexes with two thiosemicarbazide derivatives. This is to gain more information about related structural and spectral properties as well as their anticancer activities which are shining from the literature for similar compounds especially with Cu(II) and Mn(II).

EXPERIMENTAL

Materials. All the chemicals used are of analytical grade. $MnSO_4 \cdot H_2O$ and $CuSO_4 \cdot 5H_2O$ were purchased from Fluka Chemical Co.

Synthesis of oxazolinone thiosemicarbazide derivative (HL^1 and HL^2). 5-Benzylidene-3-(4-chloro-phenyl)-6-oxo-5,6-dihydro-1*H*-[1,2,4]triazine-2-carbo-thioic acid amide (HL^1) and 5-(3-bromo-4-methoxy-benzylidene)-3-(4-chloro-phenyl)-6-oxo-5,6-dihydro-1*H*-[1,2,4]triazine-2-carbothioic acid amide (HL^2) were prepared by mixed of oxazolinone and 3-bromo-4-methoxy-benzylidene derivatives (0.01 mol) and thiosemicarbazide (0.01 mol) in acetic acid (30 mL) and heated under reflux for 2 h, then cooled. The solid obtained was filtered off, washed with ethanol, dried and purified by acetic acid to give HL^1 and HL^2 (Scheme 1) as yellow crystals, yield ~ 78 %, mp 200°C.

Synthesis of metal ion complexes. A mixture of hot DMF solution (20 mL) of free 5-benzylidene-3-(4-chlorophenyl)-6-oxo-5,6-dihydro-1*H*-[1,2,4]triazine-2-carbothioic acid amide (HL^1) and 5-(3-bromo-4-meth-

oxybenzylidene)-3-(4-chloro-phenyl)-6-oxo-5,6-dihydro-1*H*-[1,2,4]triazine-2-carbothioic acid amide (HL^2) ligands (2 mmol) and hot aqueous solution (10 mL) distilled water of (1.0 mmol) each copper(II) and manganese(II) sulphate salts was refluxed for 2–3 h at 60–70°C. The resulting solutions are allowed to stand over night, a colored of Cu(II) and Mn(II) complexes were aggregated. The solid powders complexes are filtered off washed with ethanol and dried over $CaCl_2$. The purity of the complexes was checked by TLC.

Physical measurements. Microanalyses were conducted using an elemental analyzer 1106 in the Micro-analytical Unit at the Faculty of Science, Ain Shams University, Egypt. Melting points were determined on MEL–TEMP II melting point apparatus and incorrect. The metal content was determined using complexometric titrations and the sulfate ions was tested gravimetrically using $BaCl_2$ [34]. IR spectra were recorded on a Perkin–Elmer 1420 Spectrometer and a Biorad FTS 7 (KBr) in (4000–400 cm^{-1}) mid range. The UV–Vis spectra were determined in the DMSO solvent with concentration (1.0×10^{-3} M) for the free ligands and their Cu(II)/Mn(II) complexes using Jenway 6405 Spectrophotometer with 1cm quartz cell, in the range 200–800 nm. Molar conductance were measured using Jenway 4010 conductivity meter for the freshly prepared solutions at 1.0×10^{-3} mol in DMSO solvent. NMR spectra were recorded on a General Electric QE 300 instrument and chemical shifts were given with respect to TMS. Mass spectra were recorded on Gc/MS with CI (chemical imization) and a Hewlett–lackard MS–Engine Thermo-sprary and ionization by electron impact to 70 eV. The accelerating voltage was 6 KV; the temperature of the ion source was ~200°C and the emission current ~100 mA. Thermogravimetric and its differential analysis (TGA, DTG, DTA) were carried out in dynamic nitrogen atmosphere (30 mL/min) with a heating rate of 10°C/min using a Shimadzu TGA-50H thermal analyzer.

Evaluation of cytotoxic effects of certain chemical compound. Evaluation of cytotoxic effects of certain chemical compound operated in the Regional Center for Mycology and Biotechnology, Al-Azhar University, Egypt. Mammalian cell lines: MCF-7 cells (human breast cancer cell line were obtained from VACSERA Tissue Culture Unit. Chemicals Used; Dimethyl sulfoxide (DMSO), crystal violet and trypan blue dye were purchased from Sigma (St. Louis, Mo., USA). Fetal Bovine serum, DMEM, RPMI-1640, HEPES buffer solution, L-glutamine, gentamycin and 0.25% Trypsin-EDTA were purchased from Lonza. Crystal violet stain (1%): It composed of 0.5% (w/v) crystal violet and 50% methanol then made up to volume with ddH_2O and filtered through a Whatmann no. 1 filter paper. Cell line Propagation: The cells were propagated in Dulbecco's modified Eagle's medium (DMEM) supplemented with 10% heat-inactivated fetal bovine serum, 1% L-glutamine, HEPES buffer and 50 μg/mL gentamycin. All cells were maintained at 37°C in a humidified atmosphere with 5% CO_2 and were subcultured two times a week. Cell toxicity was monitored by determining the effect of the test samples on cell morphology and cell viability. Cytotoxicity evaluation using viability assay: For cytotoxicity assay, the cells were seeded in 96-well plate at a cell concentration of 1×10^4 cells per well in 100 μL of growth medium Fresh medium containing different concentrations of the test sample was added after 24 h of seeding. Serial two-fold dilutions of the tested chemical compound were added to confluent cell monolayers dispensend into 96-well, flat-bottomed microtiter plates (Falcon, NJ, USA) using a multi-channel pipette. The microtiter plates were incubated at 37°C in humidified incubator with 5% CO_2 for a period of 48 h. three wells were used for each concentration of the test sample. Control cells were incubated without test sample and with or without DMSO. The little percentage of DMSO present in the wells (maximal 0.1%) was found not to affect the experiment. After incubation of the cells for 24 h at 37°C, various concentrations of sample (50, 25, 12.5, 6.25, 3.125, and 1.56 μg) were added, and the incubation was continued for 48 h and viable cells yield was determined by a colorimetric method. In brief, after the end of the incubation period, media were aspirated and the crystal violet solution (1%) was added to each well for at least 30 minutes. The stain was removed and the plates were rinsed using tap water until all excess stain is removed. Glacial acetic acid (30%) was then added to all wells and mixed thoroughly, and then the absorbance of the plates were measured after gently shaken on Microplate reader (TECAN, Inc.), using a test wavelength of 490 nm. All results were corrected for background absorbance detected in wells without added stain. Treated samples were compared with the cell control in the absence of the tested compounds. All experiments were carried out in triplicate. The cell cytotoxic effect of each tested compound was calculated [35, 36].

Table 1. Analytical and physical data for HL^1, HL^2 ligands and their metal complexes

Compound	M_w	mp, °C	Color	Λ, Ω^{-1} cm^2 mol^{-1}	Elemental analysis							
					Found, %				Calculated, %			
					C	H	N	M	C	H	N	M
HL^1	356.83	160	Yellow	34	56.97	3.63	15.60	–	57.22	3.67	15.70	–
HL^1–Cu·3H_2O	927.31	195	Olive green	29	43.86	4.00	11.94	6.59	44.04	15.70	12.08	6.85
HL^2	465.75	210	Yellow	34	46.16	2.87	11.87	–	46.42	3.03	12.03	–
HL^2–Cu·6H_2O	1199.20	>230	Dark green	34	35.30	3.25	9.13	5.11	36.06	3.36	9.34	5.30
HL^2–Mn	1082.50	>230	Pale yellow	31	39.93	2.49	9.91	4.96	39.94	2.61	10.35	5.08

Table 2. Assignments of main IR spectral bands of HL^1, HL^2 ligands and their metal complexes

Compound	IR spectra, ν, cm^{-1}					
	ν(NH_2)	ν(NH)	ν(C=O)	ν(C=N)	ν(C=C)	ν(C=S)
HL^1	3405 3188	3285	1683	1633	1596 1520	1356
HL^1–Cu·3H_2O	3402 3188	3298	1652	1630	1487	1350
HL^2	3379	3146	1784 1694	1631	1589 1545	1362
HL^2–Cu·6H_2O	3421	–	1784	1645	1589	–
HL^2–Mn	3412	–	1784	1648	1590	–

RESULTS AND DISCUSSION

The 5-benzylidene-3-(4-chloro-phenyl)-6-oxo-5,6-dihydro-1*H*-[1,2,4]triazine-2-carbothioic acid amide (HL^1) and 5-(3-bromo-4-methoxy-benzylidene)-3-(4-chloro-phenyl)-6-oxo-5,6-dihydro-1*H*-[1,2,4]triazine-2-carbothioic acid amide (HL^2) free ligand and their metal [Cu(II) and Mn(II)] complexes were subjected to elemental analyses. The results of elemental analyses (C, H, N, and M) with molecular formula molar conductivity, color, and melting points are presented in Table 1. The results obtained are in good agreement with those calculated for the suggested formula. The structures of the ligand and metal complexes are also confirmed by IR, Mass and ^{1}H NMR spectra, which are discussed below.

Infrared spectra. The diagnostic IR spectral bands of the HL^1, HL^2, and their complexes are presented in Table 2, together with their tentative assignments. The IR spectral data containing the respective vibrational bands of the Cu(II) and Mn(II) complexes are listed in Table 2. The IR spectrum of free HL^1 and HL^2 ligands show a different intense from weak-to-very strong absorption bands at (3405 and 3188 cm^{-1}) and 3379 cm^{-1} due to ν(NH_2), respectively. The bands appear at 1356 and 1362 cm^{-1} were assigned to thioamide vibrations [37, 38] for HL^1 and HL^2, respectively. Furthermore, both ligands are expected to undergo thione ↔ thiol tautomerism. However, the appearance of distinguish thioamide bands in HL^1 and HL^2 ligands indicates the existence of both ligands in the thione form. The weak-to-medium weak bands at 3285 and 3146 cm^{-1} were assigned to ν(NH) vibrational bands for HL^1 and HL^2, respectively. The refereed bands at 1683 and 1784 cm^{-1} assigned for the vibration motions of ν(C=O) bands for HL^1 and HL^2, respectively. Also, an intense band at around 1630 cm^{-1} assigned for ν

(C=N) of the triazine ring. The aromaticity bands of ν (C=C) for both phenyl rings exhibited within range 1520–1596 cm^{-1}. A comparison between the spectra of investigated complexes with the spectrum of free ligands reflects the mode of coordination of both ligands towards metal ions. The IR spectrum of Cu(II)–HL^1 complex shows the following bands suffer shifts in appearance due to the coordination of –NH and sulfur of C=S sites. The lower shifted for both ν (C=O) and ν(C=C) vibration bands upon the located of carbonyl group beside the chelation place and also the change of electronic configuration after the complexation state. The higher shift of ν(NH) band and the lower shift of thio amide bands especially the ν(C=S) (1356 cm^{-1}) proposed their participation in coordination. The chelation mode of the HL^2 towards Cu(II) and Mn(II), displays the following significant bands at: 3379, 3146, 1784, 1631, and (1589 and 1545) cm^{-1} assigned for ν(NH_2), ν(NH), ν(C=O), ν(C=N), and ν(C=C). Also, the main significant band at 1362 cm^{-1} assigned for thioamide group. This appearance also, supports the presence of the free ligand in thione form. The IR spectrum of Cu(II) and Mn(II)–HL^2 complexes displays the same significant bands which are faraway from coordination with central atom as: 1784, 1646, and 1590 cm^{-1} assigned for ν(C=O), ν(C=N), and ν(C=C), respectively. The wavenumber of stretching ν(NH_2) band suffer higher shift in its position in Cu(II) and Mn(II) complexes at 3421 and 3412 cm^{-1} assigned for nitrogen of NH_2 group uncoordinated with central metal ions. The coordination place was proven through the absence of appearance of ν(NH) and ν(C=S) band at 3146 and 1362 cm^{-1}, respectively (free HL^2 ligand) in both Cu(II) and Mn(II)–HL^2 complexes considered the sharing of –NH and C=S in chelation process. The ν (M–S) cannot easily detect in this scanning range but proposed based on elemental analysis and conductivity measurements.

Molar conductivity. The molar conductivity values of Cu(II)–HL^1, Cu(II)–HL^2, and Mn(II)–HL^2 complexes (Table 1) were found to be in the range of 29–34 $\Omega^{-1}\,cm^2\,mol^{-1}$. These relatively low values indicate the non–electrolytic nature of these complexes [39]. The neutrality of the complexes can be accounted by both the deprotonated nature of the ligand with most complexes and the attaching of SO_4 covalently the metal ions.

Electronic spectra . A comparison of the electronic spectra of the free HL^1 and HL^2 ligands with those of their corresponding Cu(II) and Mn(II) complexes show some shifts that can be considered as evidence for the complex formation. These bands appeared in neutral medium for the free ligands at ~285 and 415 nm. These bands may be attributed to π→π* and *n*→π* transitions inside the ligands function groups. Additionally, the absorption spectra (in DMSO) of metal complexes show additive bands at different wavelengths. The absorption spectrum of Mn(II)–HL^2 complexes display medium-to-weak absorption bands at; 23525, 27174, and 34482 cm^{-1} in each complex, respectively are characteristic for octahedral geometry. These bands may be assigned as $^6A_{1g} \rightarrow {}^4E_{1g}$, $^4A_{1g}(^4G)$, $^6A_{1g} \rightarrow {}^4E_g(^4D)$, and $^6A_{1g} \rightarrow {}^4T_{1g}(^4P)$ transitions, respectively [40]. The electronic spectra of Cu(II)–HL^1 and Cu(II)–HL^2 complexes exhibit two bands at around 15267 and 21739 cm^{-1}, assigned to the transition $^2B_{1g} \rightarrow {}^2E_g$ and $^2B_{1g} \rightarrow {}^2B_{2g}$, respectively. These bands suggested distorted octahedral geometry around Cu(II) [40]. The bonding sites of Cu(II) and Mn(II) complexes are proposed in Fig. 1.

Mass spectra. The mass spectrum of 5-benzylidene-3-(4-chloro-phenyl)-6-oxo-5,6-dihydro-1*H*-[1,2,4]triazine-2-carbothioic acid amide (HL^1) compound showed an intense molecular ion peak at *m/z* 356, corresponding to the molecular formula $C_{17}H_{13}N_4ClOS$. The molecular ion of compound HL^1 (Scheme 2) underwent fragmentation to produce a peak at *m/z* 297 by losing NHCS group. The loss of NH group from the ion with *m/z* 297 resulted in an ion at *m/z* 282, which lost carbonyl group (CO) to give peak at *m/z* 254. The ion at *m/z* 254 underwent fragmentation to produce a stable peak at *m/z* 117. The ion at *m/z* 117 underwent loss of hydrogen cyanide (HCN) and acetylene molecule to give peaks at *m/z* 90 and 64. Also the ion at *m/z* 254 underwent fragmentation with rearrangement to produce peak at *m/z* 139. The ion at *m/z* 139 underwent loss of hydrogen atom, hydrogen cyanide and chlorine atom to give peaks at *m/z* 158, 111, and 76, respectively.

HL^1. Mass spectrum, *m/z* (I_{rel}, %): 358 [M^+ + 2] (3.10), 357 [M^+ + 1] (3.20), 356 [M^+] (7.70), 355 [M^+ – 1] (5.60), 340 (2.70), 339 (7.90), 338 (5.40), 299 (3.40), 298 (3.40), 297 (9.40), 296 (7.50), 284 (14.80), 283 (12.20), 281 (17.10), 204 (1.00), 203 (1.70), 197 (1.30), 195 (3.20), 194 (1.80), 179 (1.30), 178 (1.20), 177 (1.10), 176 (1.30), 155 (7.80), 154 (3.60), 153 (24.10), 152 (2.70), 141 (5.20), 140 (16.70), 139 (13.70), 138 (44.40), 137 (20.20), 119 (1.40), 118 (9.90), 117 (100.00), 116 (23.20), 105 (1.70), 104

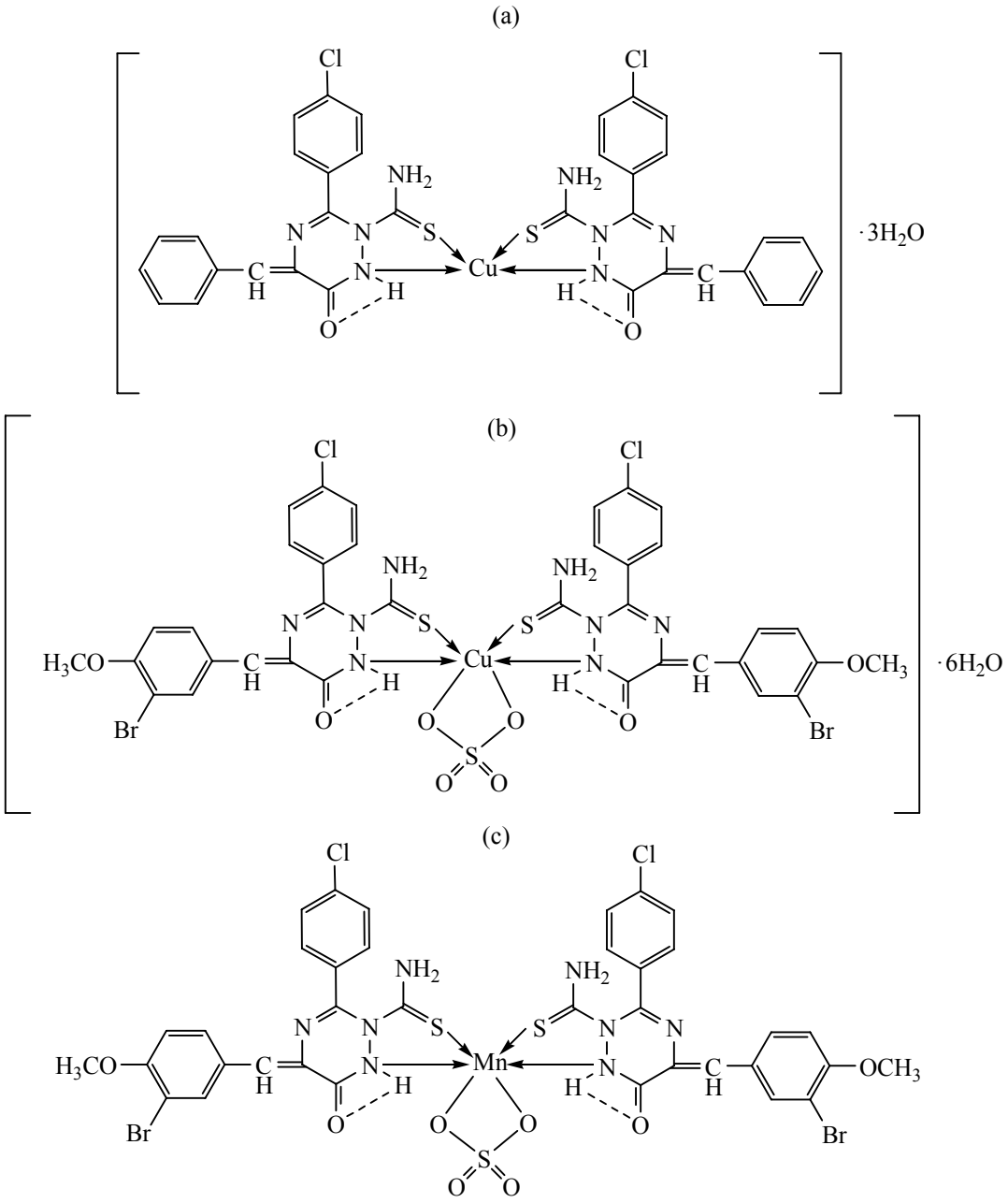

Fig. 1. The proposed structures of the HL^1 and HL^2 complexes: (a) HL^1–Cu·$3H_2O$, (b) HL^2–Cu·$6H_2O$, and (c) HL^2.

(2.80), 103 (6.10), 101 (4.80), 100 (2.20), 91 (4.40), 90 (23.90), 89 (27.60), 77 (6.50), 76 (24.30), 75 (38.40), 74 (9.70), 65 (4.80), 64 (34.30), 63 (14.10), 51 (15.50) and 50 (15.80).

The parent ion peak and the fragmentation pathway obtained through cleavage in different positions in the molecule are shown in Scheme 2. The mass spectrum of its Cu(II) complex doesn't display a peak refers to molecular ion peak. This may reflect the sudden fragmentation during the evaporation process. This is may be due to a cleavage happened to an organic part surrounds the metal ion. The first peak at *m/z* = 417 by 12% intensity which is lower intensity than known for molecular ion peak. The lower intensity gives an idea of stability of the fragment except the base peak. The base peak at *m/z* = 139 (the final fragment at *m/z* = 62) may be attributed to Cu ion. Also, the lower mp (195°C) of both HL^1 and its complex goes in a parallel with its behavior in mass spectral analysis reflecting the

Scheme 2. Main fragmentation pathways of compound HL^1

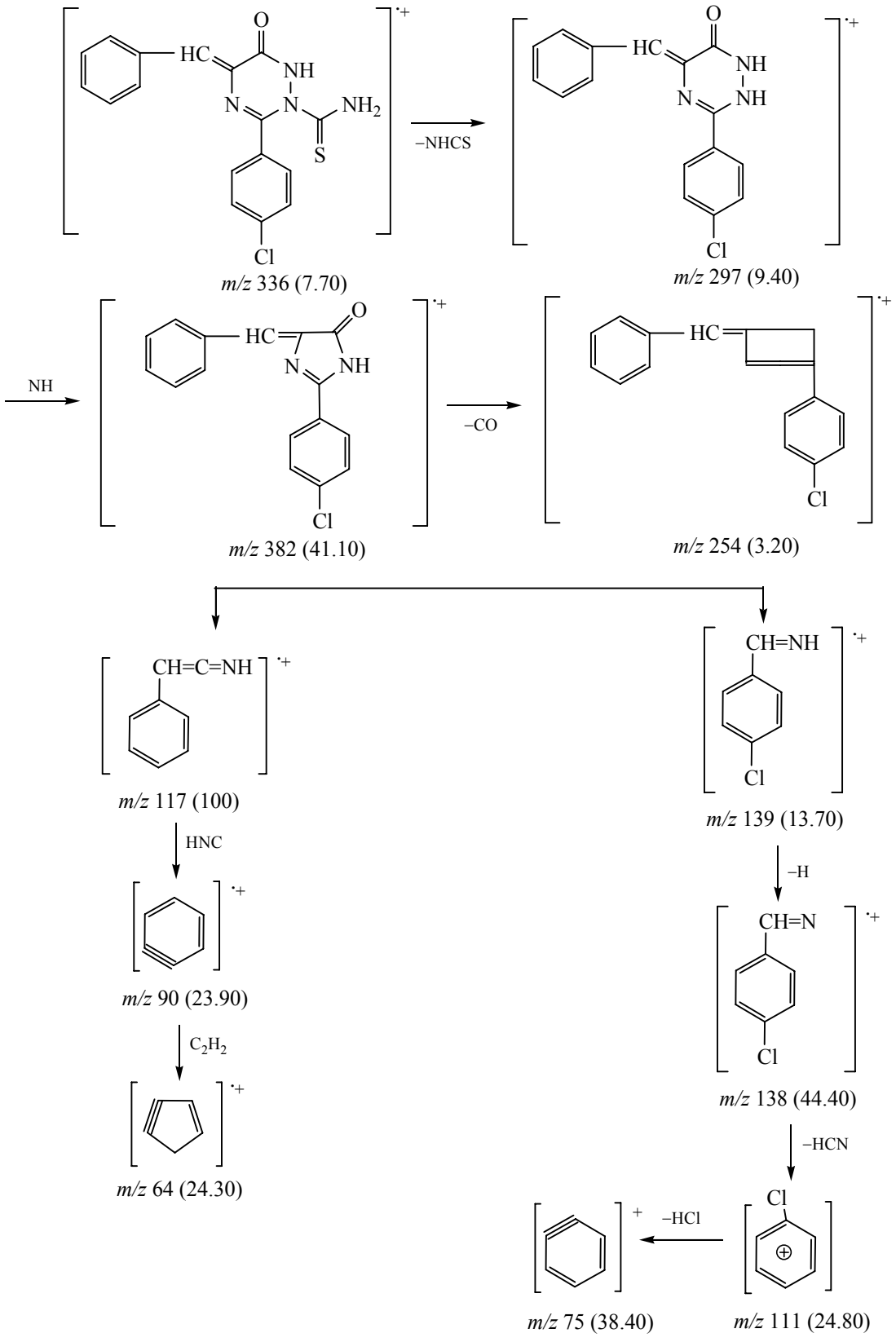

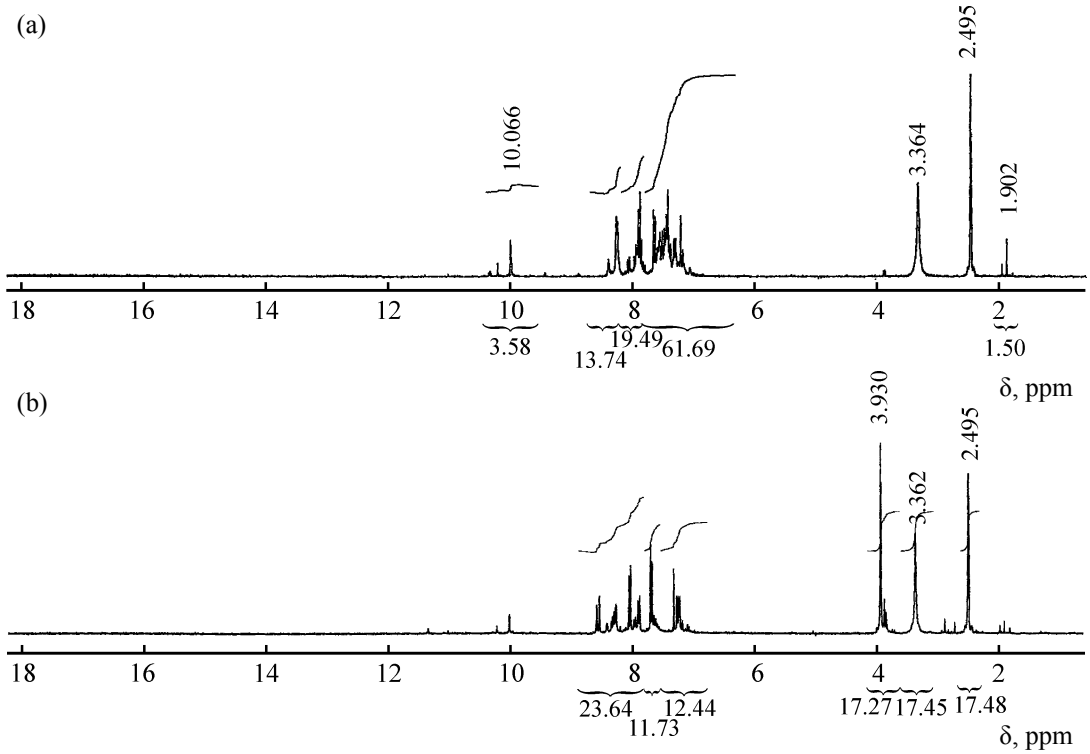

Fig. 2. ^{1}H NMR spectra of (a) HL^1 and (b) HL^2.

relative instability nature. This spectrum is not used at all as a further support for the molecular formula for this complex, but the base peak assigned for one Cu(II) ion supports the mononuclear complex proposed.

^{1}H NMR spectra. A literature survey reveals that the NMR spectroscopy has been proved useful in establishing the structure and nature of many ligands and their diamagnetic complexes. The ^{1}H NMR spectra (Figs. 2a, 2b) were recorded in DMSO-d_6 solution using Me_4Si (TMS) as internal standard. The proton magnetic resonance spectrum of HL^1 and HL^2 shows the existence of it in its thione form. **HL^1**: ^{1}H NMR spectrum (DMSO–d_6), δ, ppm: 3.36 s (2H, NH_2), 7.24–8.01 m (10H, Ar-H and H-olefinic), 8.34 s (1H, CH=N), 10.06 s (1H, NH). **HL^2**: ^{1}H NMR spectrum (DMSO–d_6), δ, ppm: 3.36 s (2H, NH_2), 3.93 s (3H, OCH_3), 7.24–8.08 m (10H, Ar-H and H-olefinic), 8.63 s (1H, CH=N), 10.06 s (1H, NH).

Molecular modeling. An attempt to gain a better insight on the molecular structure of the ligand and its complexes geometry optimization and conformational analysis has been performed by the use of MM^+ force field as implemented in hyperchem 7.5 [41]. The modeling structures of the free ligands display the stable stereo structure includes the lowest energy level (total energy 3.229 of HL^1 and total energy = 9.582 kcal/mol of HL^2) in between others may be proposed. This arrangement of sites welling to coordination may support the mode of coordination proposed in the investigated complexes.

Thermo gravimetric analysis. The thermal decomposition curves (TG/DTG and DTA) are given in Figs. 3a–3d while the TG weight loss data, DTG and DTA peak temperatures are discussed as follows:

The HL^1 ligand shows a five step of degradations. The first stage starts around 30°C and terminates at 100°C. For this stage DTG and DTA peaks appear at 53, and 55°C, respectively with closely matching data. Organic species evolve, i.e., $C_{11}H_{13}ClN_4OS$. This stage accounts for 81.71% weight loss. The first stage comes to an end around 800°C. The overall calculated mass loss is 79.82%. There is four DTA and five DTG peaks at (55, 246, 383, and 576°C) and (53, 157, 214, 317, and 570°C) for these stages. The whole degradation process leaves few carbon residues. The pyrolysis of the ligand proceeds in the following pathway:

$$C_{17}H_{13}ClN_4OS \rightarrow C_{11}H_{13}ClN_4OS \uparrow + 6\ C\downarrow \text{ (Stage I–VI).}$$

The complex, HL^1–Cu, starts to lose around 30°C. The first stage 25–83°C which accounts for 3.13% weight loss is attributed to the loss of two water

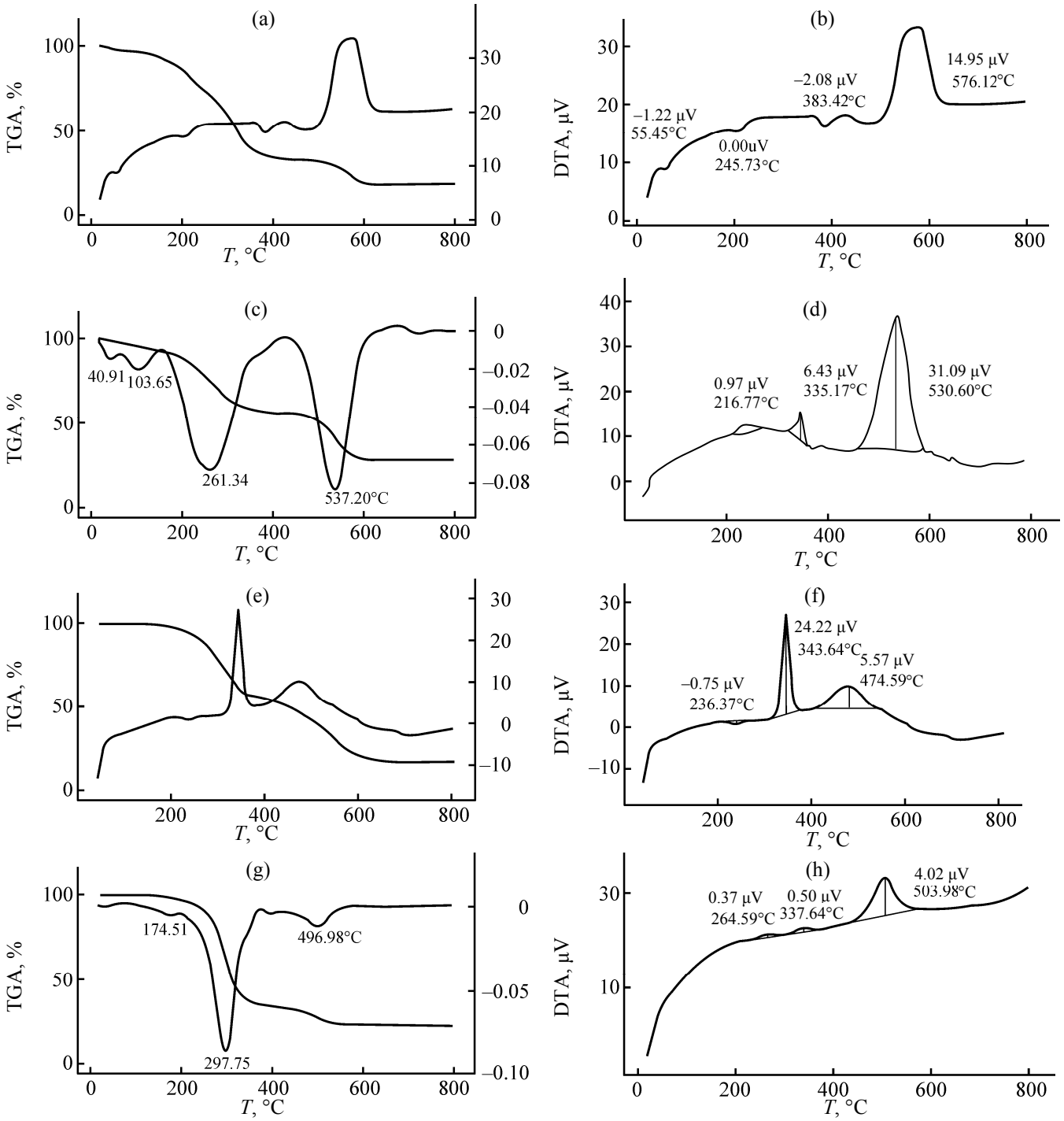

Fig. 3. TG, DTG, and DTA curves of (a, b) HL^1, (c, d) HL^1–Cu, (e, f) HL^2–Cu, and (g, h) HL^2–Mn.

molecules (outside the coordination sphere) leaving behind only one water molecules. A single medium peak for DTG at 104°C was assigned to liberate one water molecule and one chloride ions, substantiates the TG results. The remaining complex begins decomposing from 83 and up to 632°C the partially structure is destroyed. In this stage, many small gases molecules are liberated. For this step, two DTG peaks

(261, 537°C) and three DTA peaks [217 (exo), 335 (exo), 531°C (exo)] are observed which clearly show that at least three intermediates steps are also formed during this degradation stage. This stage accounts for (found 64.63%; calculated 63.00%) weight loss. The final residue that is stable after 632°C is identified as CuO polluted with carbon atoms. The three decomposition stages are summarized as follow:

$$C_{34}H_{32}Cl_2CuN_8O_9S_3 \rightarrow C_{34}H_{28}Cl_2CuN_8O_7S_3 + 2H_2O \quad \text{(Stage I)},$$

$$C_{34}H_{28}Cl_2CuN_8O_7S_3 \rightarrow C_{34}H_{26}ClCuN_8O_6S_3 + H_2O + Cl \quad \text{(Stage II)},$$

$$C_{34}H_{26}ClCuN_8O_6S_3 \rightarrow C_{34}H_{17}ClN_8O_5S_3 + CuO + 9C \quad \text{(Stage III)}.$$

The complex, HL^2-Cu, starts loosing mass around 116°C and shows a two decomposition steps. These steps have two DTG (307, 547°C) and three DTA [236 (endo), 344 (exo), 475°C (exo)]. It is interesting to note that in complexation with copper, the ligand decomposes in two steps, however, when decomposition alone, it pyrolyzed in four steps. The first stage which accounts for 42.26% weight loss is attributed to the loss of half organic moiety of HL^2 ligand leaving behind the other organic part attached with copper ions. At the second decomposition steps the ligand from work splits in unusual fashion and decomposed with 41.18% mass loss. The final residual product of Cu(II) complex is copper oxide, CuO contaminated with few carbon atoms. The thermal stability of Cu(II) complex started at 800°C and route of decomposition mechanism as follows:

$$C_{36}H_{40}Br_2Cl_2CuN_8O_{14}S_3 \rightarrow C_{14}H_{20}BrClN_4O_7S + C_{12}H_{20}BrClCuN_4O_7S_2 \quad \text{(Stage I)},$$

$$C_{12}H_{20}BrClCuN_4O_7S_2 \rightarrow C_2H_{20}BrClN_4O_6S_2 + CuO\downarrow + 10C\downarrow \quad \text{(Stage II)}.$$

The complex, HL^2-Mn, begins losing mass around 149°C. The first decomposition step at DTG (175°C) shows a mass loss of 3.17% assigned to the elimination of one methoxy molecule. This stage has a wide ends around 187°C and is marked by one DTA peak 265°C (exo). The second decomposition step which commences at 265°C and terminates at 323°C, shows a large mass loss of 61.49% assigned to decomposition of HL^2 moieties. Single peaks, each for DTG (298°C) and DTA [338°C (exo)], are found in this region. The third stage exhibits a mass loss of 11.82% in the temperature zone of 461–522°C, due to continuously destroyed framework of the manganese(II) complex. Single peaks for DTG (497°C) and DTA 504°C (exo) are observed for this stage. Above 520°C, the residue is identified as MnO_2 polluted with few carbon atoms. The equations for the degradation stages are as follows:

$$C_{36}H_{28}Br_2Cl_2MnN_8O_8S_3 \rightarrow C_{22}H_{28}Br_2Cl_2MnN_8O_8S_3 + MnO_2\downarrow + 14C \quad \text{(Stage I–III)}.$$

Kinetic studies. Different kinetic methods based on a single heating rate such as Coats–Redfern [42] and Horowitz–Metzger [43] was used to elucidate the kinetic parameters of the decomposition processes. The parameters such as activation energy E, frequency factor A, entropy change ΔS^*, enthalpy change ΔH^*, and Gibbs free energy change ΔG^* were calculated by means of the above methods (Fig. 4). The activation energy values obtained by each method were in good agreement with each other. A suitable mechanism for the thermal decomposition process of each material was also determined by means of the thermogravimetric analysis. The calculated thermodynamic parameters from TG and DTG are listed in Table 3.

Coats–Redfern equation. The equations as follow:

$$\ln\left[\frac{1-(1-\alpha)^{1-n}}{(1-n)T^2}\right] = \frac{M}{T} + B \quad \text{for } n \neq 1, \tag{1}$$

$$\ln\left[\frac{-\ln(1-\alpha)}{T^2}\right] = \frac{M}{T} + B \quad \text{for } n = 1. \tag{2}$$

Here $M = -E/R$ and $B = \ln AR/\Phi E$; each of E, R, A, and Φ are the heat of activation, the universal gas constant, pre-exponential factor and heating rate, respectively. The correlation coefficient, r, was computed using the least square method for different values of n, by plotting the left-hand side of Eqs. (1) or (2) vs $1000/T$ (Fig. 4).

Horowitz–Metzger equation. The relations derived are as follow:

$$\ln[-\ln(1-\alpha)] = \frac{E}{RT_m}\theta, \tag{3}$$

where α is the fraction of the sample decomposed at time t and $\theta = T - T_m$.

A plot of $\ln[-\ln(1-\alpha)]$ against θ, was found to be linear, from the slope of which E, was calculated and Z can be deduced from the relation:

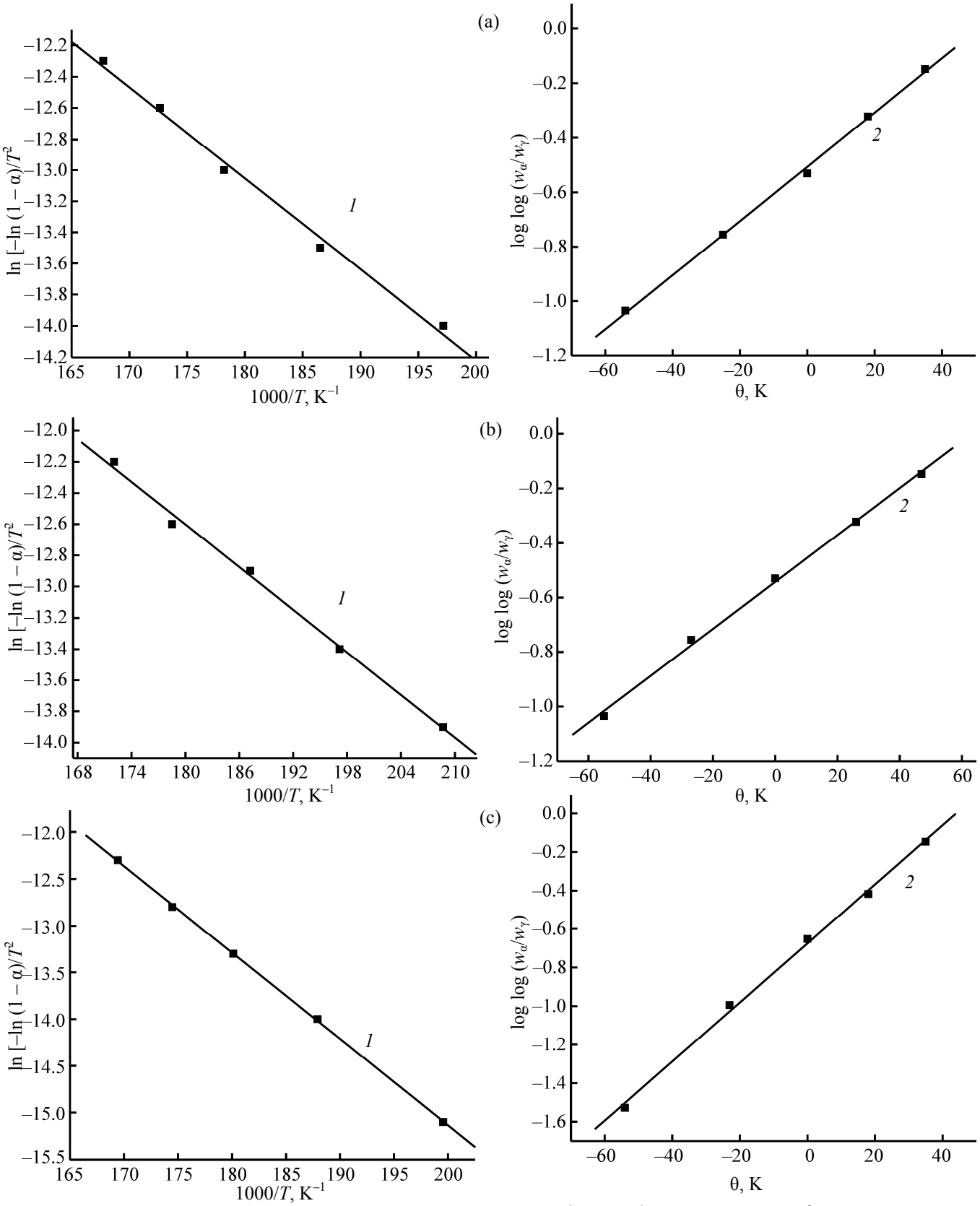

Fig. 4. (*1*) Coats–Redfern and (*2*) Horowitz–Metzger curves of (a) HL^1, (b) HL^1–Cu complex, (c) HL^2–Cu complex, and (d) HL^2–Mn complex.

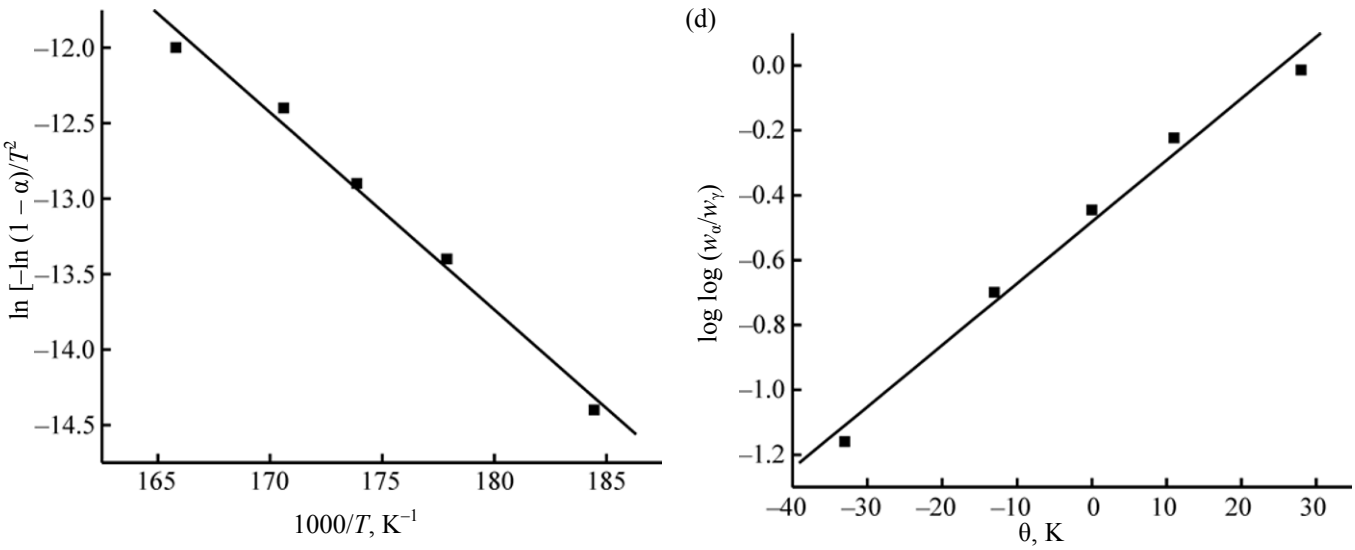

Fig. 4. (Contd.)

$$Z = \frac{E\varphi}{RT_m} \exp\left(\frac{E}{RT_m^2}\right), \quad (4)$$

where φ is the linear heating rate, the order of reaction, n, can be calculated from the following relation:

$$n = 33.64758 - 182.295\alpha_m + 435.9073\alpha_m^2 - 551.157\alpha_m^3 + 357.3703\alpha_m^4 - 93.4828\,\alpha_m^5.$$

The n value which gave the best fit ($r \approx 1$) was chosen as the order parameter for the decomposition stage of interest. From the intercept and linear slope of such stage, the A and E values were determined. The other kinetic parameters, ΔH, ΔS, and ΔG were computed using the relationships; $\Delta H = E - RT$, $\Delta S = R\ln(Ah/kT)$ and $\Delta G = \Delta H - T\Delta S$, where k is the Boltzmann's constant and h is the Planck's constant. The following remarks can be pointed out:

(1) All complexes decomposition stages show a best fit for (n = 1) indicating a first order decomposition in all cases.

(2) The negative values of activation entropies ΔS indicate more ordered activated complexes than the reactants and/or the reactions are slow.

(3) The positive values of ΔH mean that the decomposition processes are endothermic.

Cytotoxicity studies. For instance, cytotoxic and antitumor activities of prepared 5-benzylidene-3-(4-

Table 3. Kinetic parameters using Coats–Redfern (CR) and Horowitz–Metzger equations operated for HL^1 and HL^2 metal complexes

Complex	Method	Kinetic parameters					
		E, J/mol^{-1}	A, s^{-1}	ΔS, J mol^{-1} K^{-1}	ΔH, kJ/mol	ΔG, kJ/mol	r
HL^1	CR	4.86E+04	1.15E+02	–2.11E+02	4.39E+04	1.62E+05	0.99671
	HM	6.01E+04	2.23E+03	–1.86E+02	5.54E+04	1.60E+05	0.99922
HL^1–Cu·3H_2O	CR	3.79E+04	1.40E+01	–2.28E+02	3.34E+04	1.55E+05	0.99798
	HM	4.70E+04	1.97E+02	–2.06E+02	4.26E+04	1.53E+05	0.99895
HL^2–Cu·6H_2O	CR	7.68E+04	6.53E+04	–1.58E+02	7.22E+04	1.60E+05	0.99989
	HM	9.05E+04	2.87E+06	–1.26E+02	8.59E+04	1.56E+05	0.99879
HL^2–Mn	CR	1.09E+05	5.89E+07	–1.02E+02	1.04E+05	1.62E+05	0.99457
	HM	1.20E+05	9.57E+08	–7.85E+01	1.16E+05	1.61E+05	0.99279

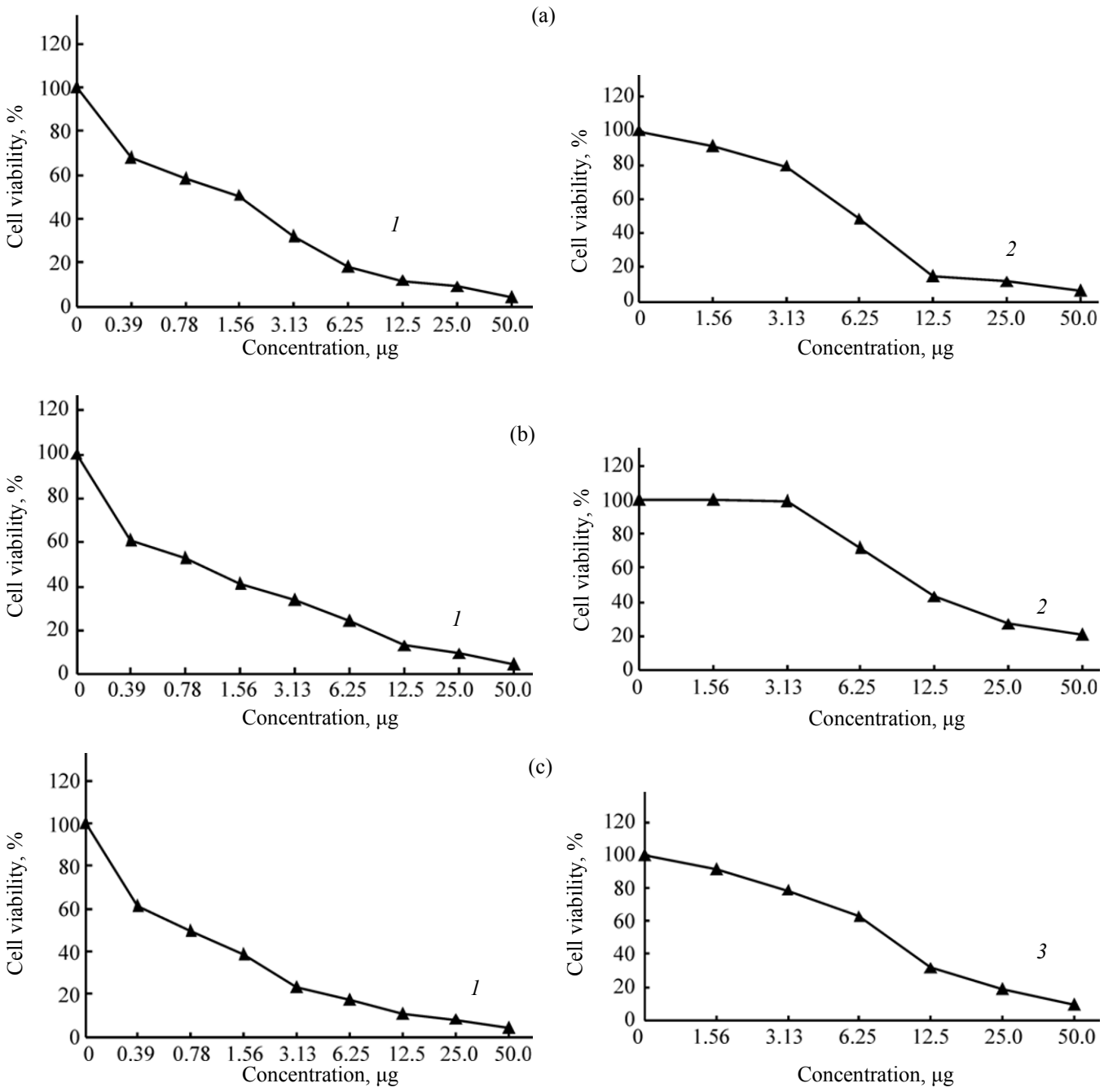

Fig. 5. Evaluation of cytotoxicity against cell line (a) HEPG-2 (b) HCT, (c) MCF-7of (*1*) HL^1 and (*2*) HL^1–Cu(II).

chloro-phenyl)-6-oxo-5,6-dihydro-1*H*-[1,2,4]triazine-2-carbothioic acid amide (HL^1) ligand and its copper(II) complex were evaluated against cell lines MCF-7, HEPG-2, and HCT according to the method of Mosmann [35]. The drug doxorubicin was used as standard. Inhibitory activity against breast carcinoma cells (MCF-7 cell line), hepatocellular carcinoma cells (HEPG-2 cell line) and colon carcinoma cells (HCT cell line) was tested by using different concentrations of the samples (50, 25, 12.5, 6.25, 3.125, 1.56, 0.78, and 0.39 μg) and cell viability (%) was determined by colorimetric method. The 50% inhibitory concentration (IC_{50}) of MCF-7 cell line was calculated from Table 4 and Fig. 5. The results of 50% inhibitory concentration

Table 4. Evaluation of cytotoxicity of HL^1 and its Cu(II) complex against MCF-7, HEPG-2, and HCT tumor cell lines

Concentration, μg	Viability of tumor type/cell line, %					
	MCF-7		HEPG-2		HCT	
	HL^1	HL^1–Cu	HL^1	HL^1–Cu	HL^1	HL^1–Cu
50	4.35	9.46	4.22	6.34	4.89	20.84
25	8.13	18.87	8.93	11.57	9.48	27.06
12.5	10.98	31.48	11.71	14.76	13.17	42.93
6.25	17.45	62.56	18.25	48.37	24.36	71.85
3.125	23.17	78.45	31.74	79.28	33.71	98.96
1.56	38.59	91.62	50.42	91.34	41.19	100.00
0.78	49.73	–	58.14	–	52.83	–
0.39	61.18	–	67.58	–	60.92	–
0	100.00	100.00	100.00	100.00	100.00	100.00

Table 5. IC_{50} (μg) values of HL^1 and its copper(II) complex after 72 h continuous exposure of tumor cell line

Compound	Tumor type/cell line		
	MCF-7	HePG-2	HCT
HL^1	0.800	1.60	1.00
HL^1–Cu	8.800	6.10	11.00
Doxorubicin standard	0.426	1.20	0.469

(IC_{50}) data are summarized in Table 5. In comparison with standard antitumor drug doxorubicin, 5-benzylidene-3-(4-chloro-phenyl)-6-oxo-5,6-dihydro-1*H*-[1,2,4]triazine-2-carbothioic acid amide (HL^1) ligand was found to be active against MCF-7, HEPG-2 and HCT cell lines. Copper(II) HL^1 complex was also found to be active against MCF-7, HEPG-2 and HCT cell line.

ACKNOWLEDGMENTS

The authors are deeply thankful to the Regional Center for Mycology & Biotechnology, Al-Azhar University, Egypt for their supported to evaluation of cytotoxic effects of certain chemical compounds operated in this study.

REFERENCES

1. Chohan, Z.H., Farooq, M.A., Scozzafava, A., and Supuran, C.T., *J. Enzyme Inhib. Med. Chem*., 2002, vol. 17, no. 1, p. 1.
2. Singh, K., Barwa, M.S., and Tyagi, P., *Eur. J. Med. Chem*., 2006, vol. 41, no. 1, p. 147.
3. Singh, K., Singh, D.P., Barwa, M.S., Tyagi, P., and Mirza, Y., *J. Enzym. Inhib. Med. Chem*., 2006, vol. 21, no. 5, p. 557.
4. Cozzi, P.G., *Chem. Soc. Rev*., 2004, vol. 33, p. 410.
5. Jarrahpour, A.A. and Zarei, M., *Molbank M377*, 2004.
6. Chandra, S. and Sangeetika, J., *J. Indian Chem. Soc*., 2004, vol. 81, no. 3, p. 203.
7. More, P.G. and Bhalvankar, R.B., *J. Indian Chem. Soc*., 2004, vol. 81, no. 1, p. 13.
8. Yildiz, M., Dulger, B., Koyuncu, S.Y., and Yapici, B.M., *J. Indian Chem. Soc*., 2007, vol. 81, no. 1, p. 7.
9. Islam, M.S., Farooque, M.A., Bodruddoza, M.A.K., Mosaddik, M.A., and Alam, M.S., *J. Biol. Sci.*, 2003, vol. 2, no. 12, p. 797.
10. Ferrari, M.B., Capacchi, S., Pelosi, G., Reffo, G., Tarasconi, P., Albertini, R., Pinelli, S., and Lunghi, P., *Inorg. Chim. Acta*, 1999, vol. 286, no. 2, p. 134.
11. Chohan, Z.H., Pervez, H., Khan, K.M., Rauf, A., and Supuran, C.T., *J. Enzyme Inhib. Med. Chem*., 2004, vol. 19, no. 1, p. 51.
12. Canpolat, E. and Kaya, M., *J. Coord. Chem*., 2004, vol. 57, no. 14, p. 1217.
13. Singh, G., Singh, Ph.A., Sen, A.K., Singh, K., Dubey, S.N., Handa, R.N., and Choi, J., *Synth. React. Inorg. Met. Org. Chem*., 2002, vol. 32, no. 1, p. 171.
14. Croot, P.L. and Hunter, K.A., *Anal. Chim. Acta*, 2000, vol. 406, p. 289; Almog, J., Hirshfeld, A., Glattstein, B., and Sterling, J., *Z. Goren, Anal. Chim. Acta*, 1996, vol. 322, p. 203.
15. Katano, H., Kuboyama, H., and Senda, M., *J. Electroanal. Chem*., 2000, vol. 483, p. 117.

16. Uma, R., Palaniandavar, M., and Butcher, R.J., *J. Chem. Soc., Dalton Trans*., 1996, vol. 10, p. 2061.
17. Zhu, B., Schechtman, S., and Chevion, M., US Patent WO 9939575, 1999.
18. Torres, E.L. and Mendiola, M.A., *Polyhedron*, 2005, vol. 24, p. 1435.
19. Singh, K., Kumar, Y., Puri, P., Sharma, C., and Aneja, K.R., *Inter. J. Inorg. Chem*., 2012, no. 2012, p. 1.
20. Mohamed, G.G., Badawy, M.A., Nassar, M.M., and Kamel, A.B., *Spect. Chim. Acta A*, 2010, vol. 77, p. 773.
21. Neunhoeffer, H., in *Comprehensive Heterocyclic Chemistry,* Katritzky, A.R. and Rees, C.W., Eds., Oxford: Pergamon Press, 1984, vol. 3, pp. 385–456.
22. Mura, P., Olby, B.G., and Robinson, S.D., *J. Chem. Soc., Dalton Trans*., 1985, no. 10, p. 2101.
23. Ghassemzadeh, M., Aghayan, M.M., and Neumuller, B., *Inorg. Chim. Acta*, 2005, no. 358, p. 2057.
24. Zhang, H.X., Kato, M., Sasaki, Y., Ohba, T., Ito, H., Kobayashi, A., and Chang, H.C., *Uosaki*, 2012, vol. 41, p. 11497.
25. Machura, B., Switlicka, A., Kruszynski, R., Mrozinski, J., Klak, J., and Kusz, J., *Polyhedron*, 2008, vol. 27, p. 2959.
26. Bereau, V., Rey, J., Deydier, E., and Marrot, J., *Inorg.Chim Acta*, 2003, no. 351, p. 389.
27. Singh, K., Barwa, M.S., and Tyagi, P., *Eur. J. Med. Chem.*, 2007, vol. 42, p. 394.
28. Singh, N.K. and Srivastava, A., *Trans. Met. Chem*., 2000, vol. 25, p. 133.
29. Wang, M., Wang, L.F., Ligands, Y.Z., and Li, Q.X., *Trans. Met. Chem*., 2001, vol. 26, p. 307
30. Li, M.X., Zhang, L.Z., Zhang, D., Ji, B.S., and Zhao, J.W., *Eur. J. Med. Chem*., 2011, vol. 46, no. 9, p. 4383.
31. Vyas, K.M., Joshi, R.G., Jadeja, R.N., Prabha, C.R., and Gupta, V.K., *Spectrochim. Acta A*, 2011, vol. 84, no. 1, p. 256.
32. Belicchi–Ferrai, M., Biscegli, F., Pelosi, G., Pinelli, S., and Traascani, P., *Polyhedron*, 2007, vol. 26, p. 5150
33. Majumder, A., Chaudrary, C.R., Mitra, S., and Dahlenburg, L., *Struct. Chem*., 2005, vol. 16, p. 611
34. Vogel, A.I., *A Text Book of Quantitative Inorganic Analysis,* London: Longman, 1994.
35. Mosmann, T., *J. Immunol. Methods*, 1983, vol. 65, p. 55.
36. Vijayan, P., Raghu, C., Ashok, G., Dhanaraj, S.A., and Suresh, B., *Indian J. Med. Res*., 2004, vol. 120, p. 24.
37. Franco, E., Lopez-Trorres, El , Mendiola, M.A., and Sevilla, M.T., *Polyhedron*, 2000, vol. 19, p. 441.
38. Nakamoto, K., *Infrared and Raman Spectra of Coordination Compounds*, New York: Wiley-Interscience, 1970.
39. Filo, J.J., Terron, A., Mulet, D., and Merno, V., *Inorg. Chim. Acta*., 1987, vol. 135, p. 197.
40. Lever, A.B.P., *Crystal Field Spectra Inorganic Electronic Spectroscopy*, 1 ed., Amsterdam: Elsevier, 1968, p. 249
41. *HyperChem Professional 7.5, Hypercube*, Inc., Gainesville, FL 32601, USA, 2002. http://www.hyper.com.
42. Coats, A.W. and Redfern, J.P., *Nature*, 1964, vol. 201, p. 68.
43. Horowitz, H.W. and Metzger, G., *Anal. Chem*., 1963, vol. 35, p. 1464.